Articleno. 4

THE CIVIL ENGINEERING JOURNAL 1-2019

INFLUENCE OF STRAINING BEAMS ON THE SEISMIC FRAGILITY OF DOUBLE-COLUMN BRIDGE PIERS

Yuye Zhang, Feng Xiao and Jahangir Badar

Department of Civil Engineering, Nanjing University of Science and Technology, Nanjing 210094, China; zyy@njust.edu.cn

ABSTRACT

The piers of girder bridges have a very important role on the safety of the structural system to earthquakes. This paper addresses the seismic fragility of double-column (DC) bridge piers by focusing on the influence of the straining beams and the direction of seismic waves. The seismic capacity of eight DC piers with different number and position of straining beams is first studied by pushover analyses. These results are used to derive empirical formulas for the seismic capacity of general DC piers and to define damage indices for prescriptive damage states. Finite element models of typical girder bridges with the different piers are carried out next to assess the seismic demand of these piers and to generate fragility curves by comparing their seismic demand and damage indices at the defined damage states. Results indicate that: (1) DC piers are more vulnerable when subjected to longitudinal ground motions compared with the case of transverse inputs; (2) the damage probability of the piers for transverse seismic inputs decreases with the increasing relative height of the straining beams; and (3) DC piers with two straining beams have enhanced performance in the transverse direction compared with those with a single straining beam.

KEYWORDS

Girder bridges; Double-column piers; Straining beams; Seismic fragility; Damage index

INTRODUCTION

Bridge structures are particularly vulnerable to damage under earthquakes and this may be responsible for significant human and economic losses [1-3]. Since the piers are one of the most susceptible components in girder bridges [4,5], the development of predictive models and design methods to account for their seismic performance is of great interest. In this paper, focus is given to the influence of the straining beams on the widely used double-column (DC) piers.

Seismic fragility analysis is an effective method available to estimate the damage level and damage probability of a bridge when subjected to potential ground motions [6,7]. The empirical fragility method is based on actual damage data from previous earthquakes [8,9], although it may not be appropriate to estimate the damage probability for specific bridge structures [10,11]. Analytical fragility curves for bridge structures where the variation of ground motions is considered as input in numerical simulations were developed for this purpose [12-14]. This method was used in recent research on bridge components and structures [15-17], and is a very promising method for assessing the seismic fragility of DC piers, particularly under transverse ground motions.

For DC piers there are significant differences on the plastic hinge mechanism that develops under longitudinal and transverse ground motions. The seismic fragility analysis is also more evolved if considering the influence of the straining beams. This paper therefore presents an evaluation method that can be used to assess the structural safety of DC piers under earthquakes

and the contribution of the straining beams to their seismic vulnerability. A typical girder bridge is selected for analysis by varying both number and position of the straining beams. The influence of the beams on the seismic fragility of the DC piers subjected to transverse seismic waves is investigated using a simplified method based on a displacement failure criterion. The damage indices for the DC piers are obtained for each seismic input direction by performing non-linear time history analyses, which are used to construct the fragility curves for five damage states and to obtain the damage probabilities. The method and results obtained in this paper could provide guidance for seismic performance assessment studies and for the seismic design of DC piers in girder bridges.

FRAGILITY ANALYSIS METHODOLOGY

The basic theory of fragility analysis

The seismic fragility analysis is based on the comparison between the seismic capacity and demand to assess if the seismic capacity of the structure is exceeded beyond a specified damage level, for a given ground motion intensity. The probability of such event can be expressed as:

$$P_f = P\left(\frac{D_d}{D_c} \geq 1 \middle| IM\right) \tag{1}$$

where P_f is the failure probability, D_d is the seismic demand on the structures, D_c is the capacity of the structure, and IM is the ground motion intensity measure.

To obtain the fragility curves, both demand and capacity of the structure need to be assessed. For this purpose, the Bayesian probabilistic seismic demand model (PSDM) can be used to obtain the structural demand, as presented by Gardoni *et al.* [18] and Ahmad *et al.* [19]. Limit states are defined as the thresholds of prescriptive damage states for the structural capacity (e.g., slight, moderate, extensive and complete damage – more details ahead) [20,21]. In this paper, the PSDM of the DC bridge piers is developed using nonlinear time-history analyses to establish a relationship between the seismic demand and the ground motion intensity. The displacement ductility ratio of the piers is selected as the engineering parameter for the limit state capacity.

Fragility analysis procedure for DC piers

The fragility analysis procedure herein proposed considers the structural characteristics of the DC piers and the different responses under longitudinal and transverse seismic inputs. It is described as follows: (1) A nonlinear model of the bridge is first established by considering the interaction between pile and soil; (2) 100 seismic records are selected from the Pacific Earthquake Engineering Research Center (PEER) – which are suitable for the type of sites considered – to formulate series of "bridge-ground motion" samples; (3) The damage indices of bridge piers for different damage states are determined based on the displacement responses corresponding to the failure states obtained by a pushover analysis. These responses are also used to assess the pier capacity and damage indices; (4) The seismic demand is then obtained by a nonlinear time history analysis using the finite element model established in Step 1; (5) The probability function of the structural response exceeding a specific damage state under different levels of ground motion is calculated; and (6) the fragility curves of DC bridge piers are plotted as a function of the selected ground motion intensities.

ANALYTICAL MODELING AND SIMULATION

Description of the bridge model

The elevation and components of the selected bridge are shown in Figure 1. The bridge has five equivalent spans of 30 m each. A continuous structural system is adopted for the bridge deck. The girders are supported by four DC piers of 30 m height and two abutments. C50 concrete, with standard compressive strength of 29.6 N/mm2, is applied to the girders, while C40 concrete (with standard compressive strength of 26.8 N/mm2) is applied to both DC piers and straining beams. The longitudinal reinforcement ratio of the column and straining beam is 0.852% and 0.485%, respectively. A fixed bearing is arranged on the middle pier, as shown in Figure 1, and movable bearings are arranged on the other piers and the abutments.

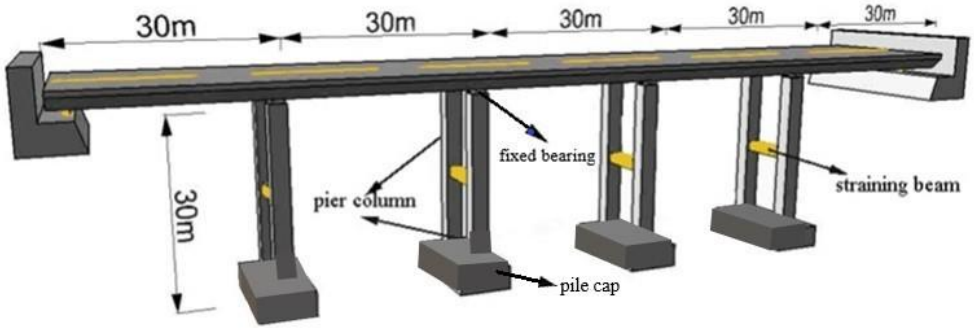

Fig. 1 -Structural layout of the bridge

The numerical model of the bridge is developed using SAP2000 software. The bridge girder is simulated using linear elastic beam elements, since the superstructure remains elastic when subjected to the seismic actions considered in this study. Elasto-plastic fiber column-beam elements are used to simulate the pier columns and straining beams. Both piers and superstructure are connected using the bearings. The piers are fixed on rigid pile caps, which in turn are connected to elements with six degrees of freedom placed under the pile cap to simulate the soil-pile-superstructure seismic interaction, as recommended by Zhang and Dias-da-Costa [3].

Details of different types of DC piers

Eight models of DC piers with different number and layout of straining beams, and direction of seismic input are herein used to assess the seismic fragility. A typical representation of the DC piers is shown in Figure 2, whereas the different variations are listed in Table 1. Figure 3 shows the cross sections of pier columns and the steel bar arrangement, in which Φ represents the diameter of the steel bar in millimetre. The longitudinal and transverse steel bars all have a yielding strength of 335 MPa.

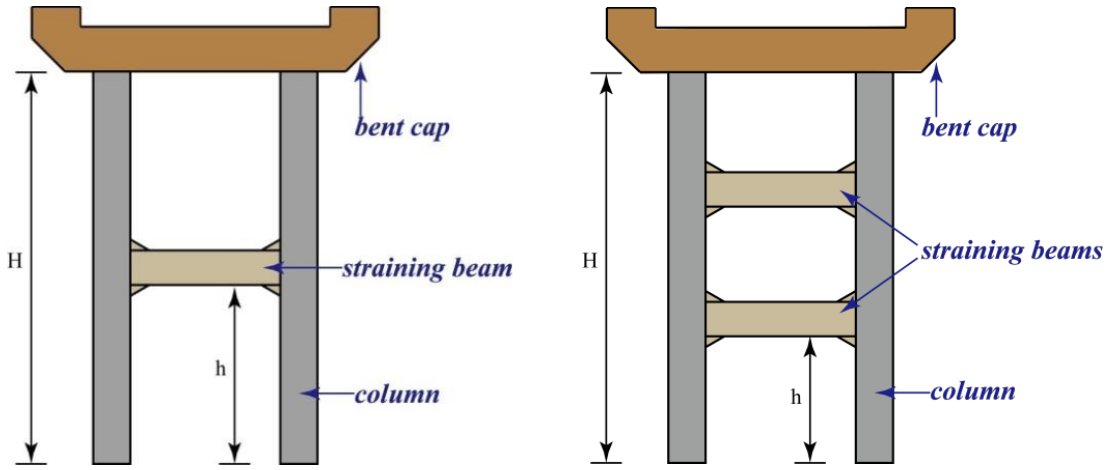

(a) With single straining beam *(b) With double straining beam*

Fig. 2 -Typical DC piers

Tab. 1 - Types of models for the DC piers

Model	Number of straining beams	Position of Straining beams (h/H)*	Seismic input direction
1	1	0.3	longitudinal
2	1	0.5	longitudinal
3	1	0.7	longitudinal
4	1	0.3	transverse
5	1	0.5	transverse
6	1	0.7	transverse
7	2	0.5 and 0.8	transverse
8	2	0.5 and 0.8	longitudinal

Notes: *H* is the height of pier column; *h* is the distance from the bottom of the straining beam to the bottom of the pier column.

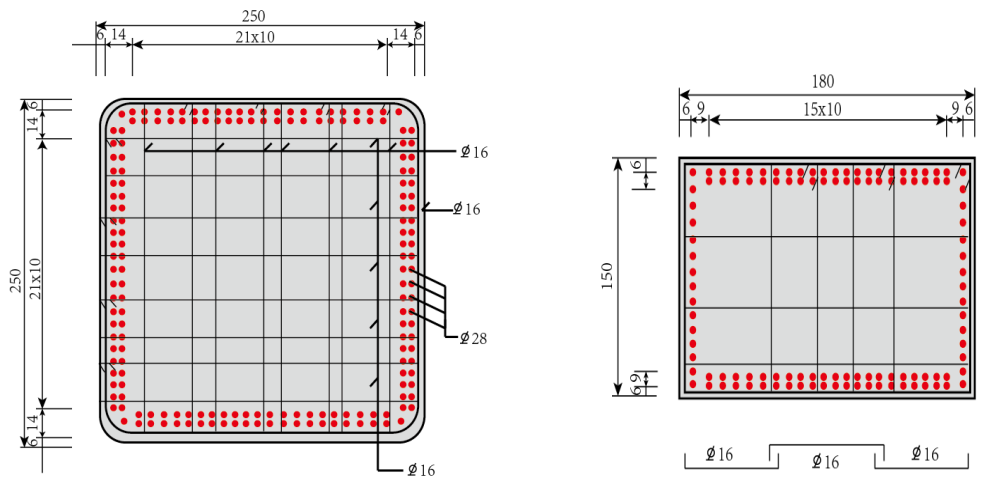

(a) Pier columns *(b) Straining beams*

Fig. 3 – Cross sections and steel bar arrangement of components (unit: cm)

Ground motion input

A total of 100 near-fault strong ground motion records are selected to conduct the seismic fragility analyses of the DC bridge piers. These records cover a wide range of values and are available from the PEER strong earthquake database. All selected ground motions have the PGA ranging from 0 to 0.8 g with epicentral distances less than 20 km. The PGA distribution and corresponding spectral accelerations are shown in Figure 4.

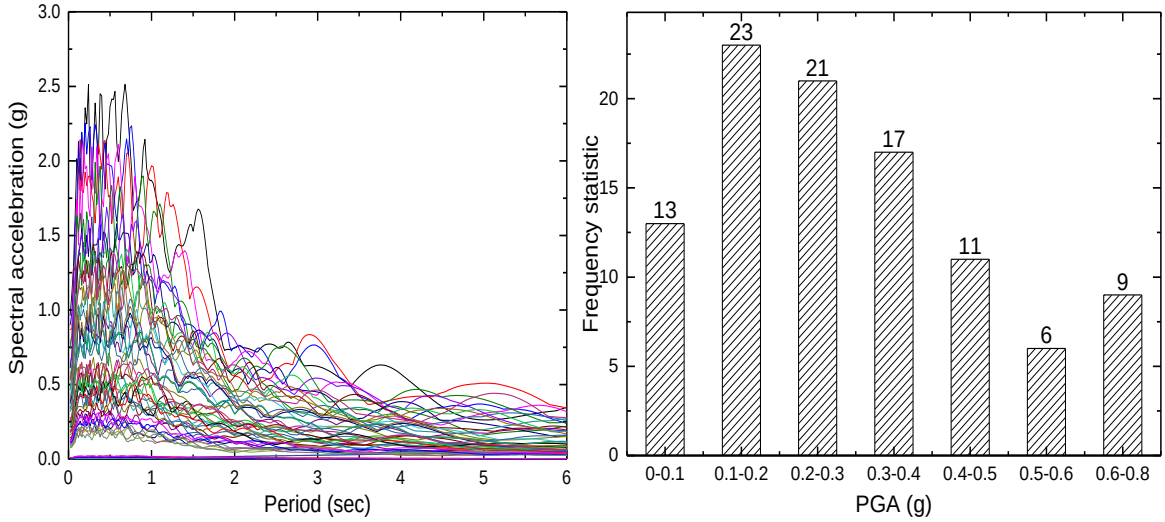

(a) Acceleration spectra *(b) PGA distribution*

Fig. 4 -Selected ground motions

CHARACTERISATION OF DAMAGE STATES

To estimate the seismic fragility of the bridges, the damage states of the structure are determined in terms of performance level by considering the relationship between the damage index and the structural capacities or limit states. In the present work, the displacement ductility of the bridge piers is used to determine five damage states, as suggested by Hwang *et al.* [22], Padgett *et al.* [23] and Zhang and Huo [24].

In the following sections, the damage index for DC bridge piers is defined using a displacement failure criterion in the longitudinal direction. The displacements corresponding to each damage state is obtained from pushover analyses carried out to assess the structural capacities of the DC bridge piers.

Damage index in the longitudinal direction

The damage indices suggested by Hwang *et al.* [22] are herein adopted for the longitudinal DC bridge piers. A relative displacement ductility ratio is used to define the following five damage states according to FEMA [20]: no damage, slight damage, moderate damage, extensive damage and complete damage. Table 2 summarises the definition of the damage states based on the displacement ductility ratio, μ_d. This parameter represents the ratio between the maximum relative displacement (Δ) and the initial yield displacement (Δ_{cy1}) according to the equation bellow:

$$\mu_d = \frac{\Delta}{\Delta_{cy1}} \tag{2}$$

Tab. 2 - Bridge damage states in the longitudinal direction

Damage state	Damage index	Description
No damage	$\mu_d \leq \mu_{cy1}$*	No damage
Sight damage	$\mu_{cy1} < \mu_d \leq \mu_{cy}$	Longitudinal reinforcement first yields
Moderate damage	$\mu_{cy} < \mu_d \leq \mu_{c4}$	Protective layer of concrete peels partly; longitudinal steel yielding; remaining components in normal use
Extensive damage	$\mu_{c4} < \mu_d \leq \mu_{cmax}$	Core concrete severely cracked; reinforcement exposed
Complete damage	$\mu_d > \mu_{cmax}$	Bridge collapses

Notes: μ_{cy1} is the displacement ductility ratio when the steel first yields; μ_{cy} is the yielding displacement ductility ratio; μ_{c4} is the displacement ductility ratio when the concrete compressive strain reaches 0.004; μ_{cmax} is the maximum displacement ductility ratio.

Damage index in the transverse direction

The method proposed above cannot be directly applied to the definition of the damage index in the transverse direction due to the dynamic axial force of the straining beams. For this purpose, 30 DC bridge piers OpenSees models with straining beams of different location are used to obtain the capacity of the pier. The location ranges in evenly incremental steps from 0.2*H* to 0.7*H*, where *H* is the height of the pier column. Models with double straining beams are also considered with their location selected between 0.5*H* and 0.7*H*. In both types of models, the displacement for which the steel bars first yield and the ductility ratio when the concrete strain reaches 0.004 are obtained.

Both pier columns and straining beams are simulated using nonlinear fiber column-beam elements. The cross-sections of the pier columns are divided into core and cover areas due to the confinement of the stirrups. Elastic elements simulate the bent-cap and the vertical load of each column is 5,600 kN, which corresponds to the weight of the superstructure above the piers.

The formula applicable to the calculation of the displacement at the top of a single column pier is given by:

$$\Delta_{cy1} = \frac{\phi_y^{'} H^2}{3} \tag{3}$$

where ϕ'_y is the yield curvature of the section, H is the height of pier column, and Δ_{cy1} is the displacement at the top of the pier when the steel within the plastic hinge region first yields.

A simplified method to obtain the elastic-plastic displacement capacity of the bent pier was proposed by Shen *et al.* [24] based on the single-column pier relation. For DC piers with one or more straining beams, a reduction factor β related with the relative position of straining beam (*h*) can account for the contribution of the straining beams to the displacement. This reduction factor can be expressed as:

$$\beta = \frac{\Delta_{cy1}^{'}}{\Delta_{cy1}} \tag{4}$$

where β is the reduction factor, Δ'_{cy1} is the top displacement of DC pier, and Δ_{cy1} is the top displacement of single-column pier.

The reduction factor can be calculated from the relationship between the top displacement of the DC piers and the single-column piers provided by pushover analyses. A summary of the analytical results (6 of 30 cases for DC pier) are listed in Table 3 and the regression analysis made based on these results is represented in Figure 5.

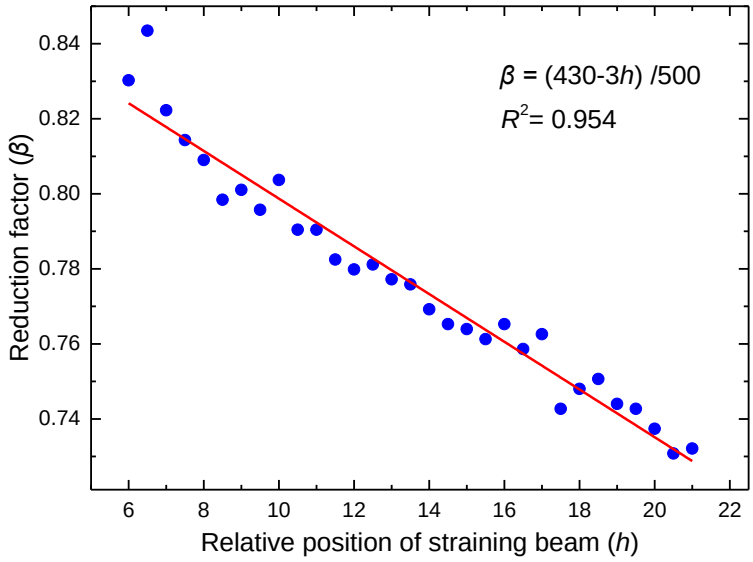

Fig. 5 -Regression analysis of the relationship between the reduction factor and straining bea Position

Tab. 3 - Displacement at the top of the pier obtained by pushover analyses (mm)

Stress state	Single-column pier	DC pier					
		0.2*H*	0.3*H*	0.4*H*	0.5*H*	0.6*H*	0.7*H*
Steel first yields	377	313	302	294	288	282	276
Concrete strain when compression reaches 0.004	1011	438	429	420	414	408	402

The regression analysis equation relates the displacement at the top of DC piers with the yielding of the steel reinforcement and the relative position of the straining beam:

$$\Delta'_{cy} = \beta\Delta_{cy} = \left(\frac{430-3h}{500}\right)\frac{\phi'_y H^2}{3} \tag{5}$$

where ϕ'_y is the yield curvature of the section, H is the height of pier column (m), and h is the distance from the bottom of the straining beam to the bottom of the pier column (m).

To predict the plastic displacement capability of the pier, it is necessary to have a reasonable estimate of the equivalent plastic hinge length. The equation suggested by Priestley *et al.* [26] is herein recovered. Accordingly:

$$L_p = 0.08H + 0.022\, f_y d_s \geq 0.04\, f_y d_s \tag{6}$$

where L_p is the length of the plastic hinge, and f_s is the characteristic strength, and d_s the diameter of the longitudinal bar.

The plastic rotation of the DC pier can then be calculated by:

$$\theta_u = L_p\left(\phi_u - \phi_y\right)/K \tag{7}$$

where θ_u is the plastic rotation, ϕ_u is the limit curvature of the cross section, ϕ_y is the equivalent yield curvature, and K is the security ductility coefficient, usually taken as 2.

Finally, the formula to calculate the capacity at the top of the DC pier is proposed as follows:

$$\Delta_u = \beta \frac{\phi_y^{'} H^2}{3} + \theta_u \left(h - \frac{L_p}{2} \right) \tag{8}$$

Determination of the damage indices

The pushover model with two straining beams (the relative height of the straining beams are 0.5*H* and 0.8*H*) has nearly the same displacements as the model with a single straining beam, when the relative height of the straining beam is 0.5*H*. Therefore, the displacement at the top of the DC pier in the first case can also be approximated by the expression for a pier with a single straining beam.

The probabilistic characteristics of the structural capacity of the bridge expressed in terms of ductility ratios can be described using a lognormal distribution [9,14]:

$$\mu_c = Ln(\tilde{\mu}_c, \beta_c) \tag{9}$$

where $\tilde{\mu}_c$ is the medium value of the structural capacity, and β_c is the logarithmic standard deviation. The median values of the structural capacity for the different damage state are listed in Table 4.

Tab. 4 - Median values for the structural capacity under different damage states

Damage state	Model 1,2,3 and 7	Model 4	Model 5	Model 6	Model 8
μ_{cy1}	1	1	1	1	1
μ_{cy}	1.23	1.23	1.23	1.23	1.23
μ_{c4}	2.69	1.42	1.44	1.47	1.44
μ_{max}	5.69	4.42	4.44	4.47	4.44

Notes: parameter definition is the same as in Table 2.

SEISMIC FRAGILITY ANALYSIS OF DC BRIDGE PIERS

Probability analysis of structural responses

The probabilistic characteristic of the structural demand can also be described by a lognormal distribution as:

$$\mu_d = Ln(\tilde{\mu}_d, \beta_d) \tag{10}$$

where $\tilde{\mu}_d$ is the medium value of the structural demand, and β_d is the logarithmic standard deviation. Both are determined from the regression of the simulated response date.

The regression analysis of the displacement ductility ratio versus PGA are shown in Figure 6 and the regression functions for all models are summarized in Table 5. It should be noted that the time history analysis are conducted using SAP2000.

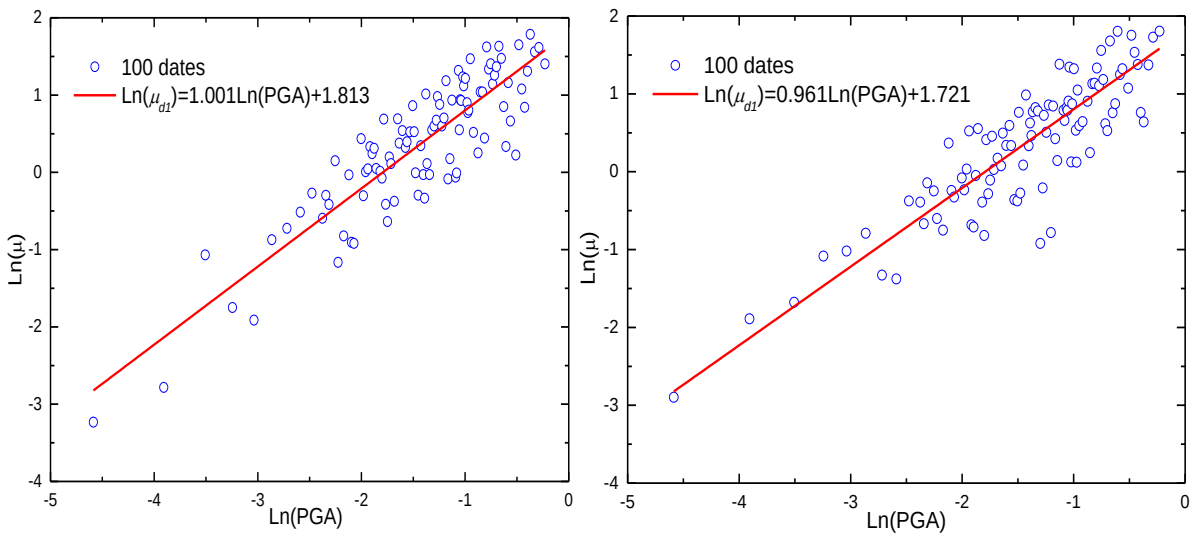

(a) Model 2 *(b) Model 5*

Fig. 6 -Regression analysis of displacement ductility ratio versus the PGA

Tab. 5 - Regression function for all pier models

Model	Seismic input	Fitting function	R^2
1	longitudinal	Ln(μ_{d1})=1.0107(PGA)+1.8129	0.8256
2	longitudinal	Ln(μ_{d2})=0.9337(PGA)+1.8037	0.7765
3	longitudinal	Ln(μ_{d3})=0.9124(PGA)+1.7769	0.8133
4	transverse	Ln(μ_{d4})=0.9724(PGA)+1.705	0.8021
5	transverse	Ln(μ_{d5})=0.9614(PGA)+1.7208	0.7854
6	transverse	Ln(μ_{d6})=0.9267(PGA)+1.6549	0.7821
7	transverse	Ln(μ_{d7})=0.9233(PGA)+1.7811	0.8377
8	longitudinal	Ln(μ_{d8})=0.9759(PGA)+1.7438	0.8189

Notes: PGA is the peak ground acceleration; R^2 is the variance.

Fragility curves of DC piers

The probability of the structure demand μ_d exceeding the capacity μ_c is described by the following equation:

$$P_f = P\left(\frac{\mu_c}{\mu_d} \le 1\right) = P\left[\ln\left(\frac{\mu_c}{\mu_d}\right) \ge 0\right] \tag{11}$$

It is highlighted that Equation (10) can be transformed into a standard normal distribution since μ_d and μ_c both follow a lognormal distribution. The equation is written as:

$$P_f = \Phi\left(\frac{-\ln(\tilde{\mu}/\tilde{\mu}_d)}{\sqrt{\beta_c^2 + \beta_d^2}}\right) \tag{12}$$

where $(\beta_c^2 + \beta_d^2)^{1/2}$ is equal to 0.5 when the PGA is selected as the intensity measure. The median values of the capacities of the components corresponding to the different failure states are listed in Table 4, whereas, the median values for the seismic demand on the piers corresponding

to the different seismic waves are shown in Table 5. The failure probability of the piers in the different conditions can be obtained from Equation (11) and the corresponding fragility curves are shown in Figure 7.

To allow more clearly comparisons of the fragility of the bridge piers in different categories, the damage probabilities of the piers along with the relative difference, $\mathcal{E}$, according to the damage likelihood of the eight models at the four damage states under 0.5 g seismic waves, are presented in Table 6. The eight piers are divided into three groups in Table 6: Group 1 consists of three piers with single straining beam subjected to longitudinal seismic waves; Group 2 consists of three piers with single straining beam subjected to transverse seismic waves; and Group 3 consists of two piers with double straining beams. It should be noticed that 'ref' identifies the pier model from each group used as reference in the calculation of the relative differences for the other piers in the same group.

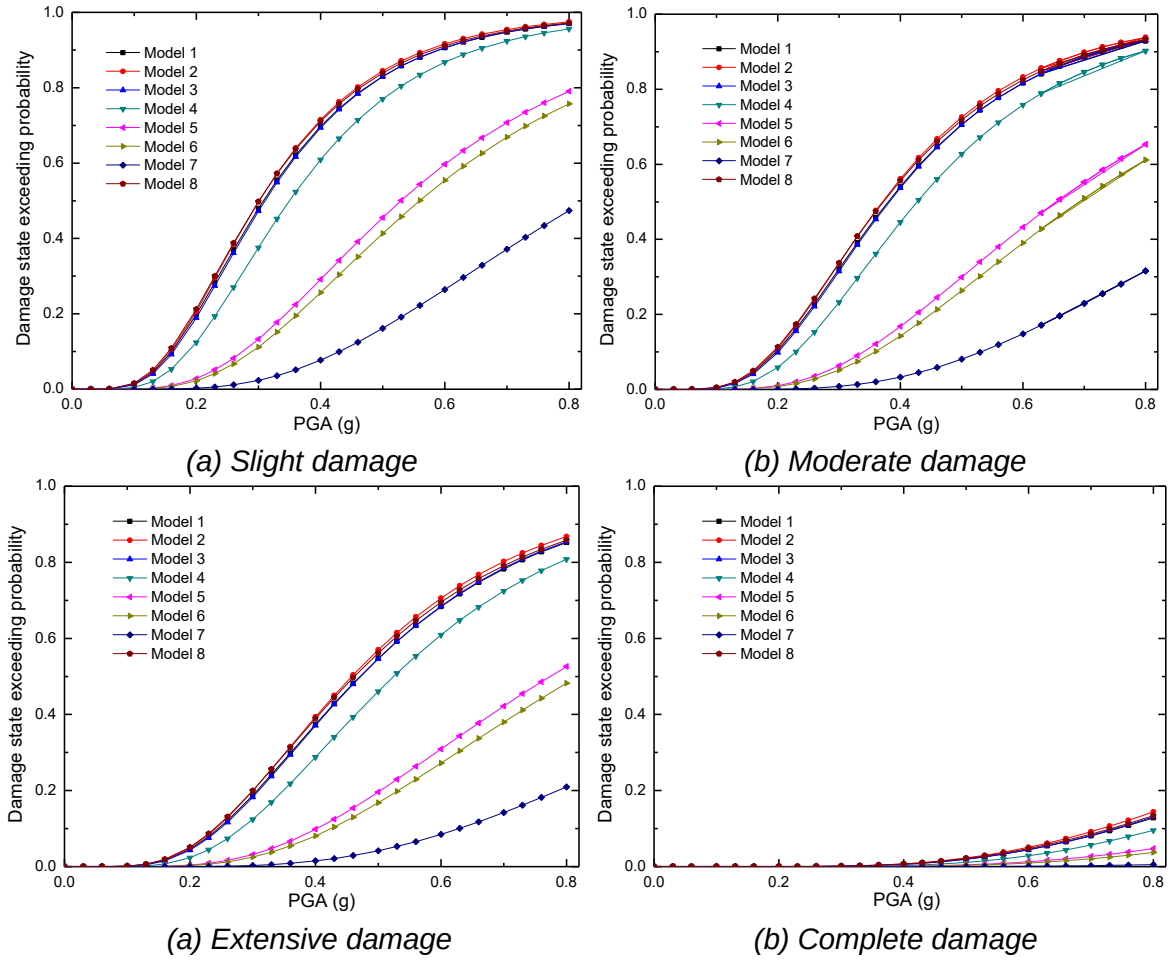

Fig. 7 -The fragility curves of DC piers for each damage state

Tab. 6 - Damage probabilities of the piers at 0.5 g

Group	Model	Damage state							
		Slight damage		Moderate damage		Extensive		Complete	
		*P**	*ℰ*	*P*	*ℰ*	*P*	*ℰ*	*P*	*ℰ*
Group 1	1	83.0%	ref	70.6%	ref	54.7%	ref	1.9%	ref
	2	84.5%	0.018	72.6%	0.028	57.0%	0.042	2.3%	0.211
	3	83.0%	0	70.5%	-0.001	54.6%	-0.002	2.0%	0.053
Group 2	4	77.0%	ref	62.7%	ref	46.1%	ref	11.0%	ref
	5	45.5%	-0.409	29.9%	-0.523	19.6%	-0.575	0.5%	-0.955
	6	41.3%	-0.464	26.3%	-0.581	16.9%	-0.633	0.4%	-0.964
Group 3	7	16.2%	-0.807	8.0%	-0.889	4.2%	-0.925	0.2%	-0.905
	8	83.9%	ref	71.8%	ref	56.1%	ref	2.1%	ref

Notes: *P* is the damage probabilities of the piers; *ℰ* is the relative differences in each group.

As can be donated from Figure 7, the probabilities of failure for the DC piers under transverse seismic inputs are smaller than those under longitudinal seismic inputs. For example, in Table 6, the damage probabilities of Models 4, 5 and 6 for the extensive damage state under transverse waves ranging from 16.9% to 46.1% are significantly smaller than those of Models 1, 2 and 3 under longitudinal waves ranging from 54.6% to 57.0%. Also from Figure 7, it can be concluded that the bridge piers with double straining beams have lower probabilities of damage under a given level of transverse earthquake intensity in comparison to a single straining beam. Taking Models 5 and 7 for example, the probabilities of slight damage of the former model is 45.5% (see Table 6), whereas the 16.2% is found in the latter. This represents a reduction of 64.4% relatively to Model 5 under 0.5 g transverse seismic input.

Regarding the influence of the position of straining beams, it is obvious from Table 6 that the damage probabilities of the piers under transverse seismic inputs decrease with the increasing relative height of the straining beams. Taking Group 2 for instance, it is observed that the moderate damage probabilities of Models 4, 5 and 6 (with h/H of 0.3, 0.5 and 0.7) are 62.7%, 29.9% and 26.3%, respectively, with the probability reducing 52.3% for Model 5 and 58.1% for Model 6, compared with that of Model 4. For the seismic fragility of DC pier under the longitudinal seismic input, it can be seen from Figure 7 that the fragility curves of Models 1, 2, 3, and 8 almost overlap. Taking the moderate damage state as example, the probabilities of Models 1, 2, 3 and 8 are 70.6%, 72.6%, 70.5% and 71.8%, respectively, in which case the maximum difference is only 2.1%. This confirms that the straining beam has reduced influence over the seismic fragility of DC piers in the longitudinal direction.

CONCLUSIONS

This paper adopts an analytical method to assess the seismic fragility of DC bridge piers with straining beams varying in number and relative position for different seismic input directions. Simplified formulas are proposed to calculate the capacity of the DC bridge piers under transverse seismic waves.

The fragility curves of DC piers with different straining beams are constructed for five damage states. Based on the obtained results, it is clear that DC bridge piers are more vulnerable to longitudinal seismic inputs than to transverse seismic inputs. The damage probability for DC piers with single straining beam under transverse seismic inputs decreases with the increasing relative location of the straining beams, with the relative position of straining beam between 0.3*H* and 0.7*H* (*H* is the height of pier column). When two straining beams are used, there is a

significant improvement of the seismic performance of DC piers in the transverse direction. These observations are particularly relevant to the design and improvement of the seismic capacity of girder bridges with DC piers, as well as to better predict their seismic performance.

ACKNOWLEDGEMENTS

The research described in this paper was supported by the National Natural Science Foundation of China (Grant No.: 51508276), and the Fund of National Engineering and Research Center for Mountainous Highways (Grant No.: GSGZJ-2017-02).

REFERENCES

[1] Nielson B.G., DesRoches R., 2007. Analytical seismic fragility curves for typical bridges in the central and southeastern united states. Earthquake Spectra, vol. 23(3): 615–633

[2] Wu F., Zhang Q., Feng B., et al., 2016. Research on the aseismic behavior of long-span cable-stayed bridge with damping effect. The Civil Engineering Journal, vol. 8: 1-9

[3] Zhang Y., Dias-da-Costa D., 2017. Seismic vulnerability of multi-span continuous girder bridges with steel fibre reinforced concrete columns. Engineering Structures, vol. 150: 451–464

[4] Ramanathan K., Desroches R., Padgett J.E., 2012 A comparison of pre- and post-seismic design considerations in moderate seismic zones through the fragility assessment of multispan bridge classes. Engineering Structures, vol. 45: 559–573

[5] Zhang K., Sun Q., 2017. Strengthening of a reinforced concrete bridge with prestressed steel wire ropes. The Civil Engineering Journal, vol. 3: 267–285

[6] Tavares D.H., Padgett J.E., Paultre P., 2012. Fragility curves of typical as-built highway bridges in eastern Canada. Engineering Structures, vol. 40: 107–118

[7] Biglari M., Ashayeri I., Bahirai M., 2016. Modeling, vulnerability assessment and retrofitting of a generic seismically designed concrete bridge subjected to blast loading. International Journal of Civil Engineering, vol. 14:379–409

[8] Yamazaki F., Motomura H., Hamada T., 2000. Damage assessment of expressway networks in Japan based on seismic monitoring. Proceedings of the 12th World Conference on Earthquake Engineering, Auckland, New Zealand

[9] Shinozuka M., Feng M.Q., Kim H.K., et al., 2000. Nonlinear static procedure for fragility curve development. Journal of Engineering Mechanics-ASCE, vol. 126(12):1287–1295

[10] Mander J.B., Basoz N., 1999. Seismic fragility curve theory for highway bridges, Proceedings of the 5th United States Conference on Lifeline Earthquake Engineering, Seattle, USA.

[11] Hwang H., Jernigan J.B., Lin Y.W., 2000. Evaluation of seismic damage to Memphis bridges and highway systems. Journal of Bridge Engineering, vol. 5:322–330

[12] Karim K.R., Yamazaki F., 2001. Effect of earthquake ground motions on fragility curves of highway bridge piers based on numerical simulation. Earthquake Engineering and Structural Dynamics, vol. 30(12):1839–1856

[13] Padgett J.E., DesRoches R., 2008. Methodology for the development of analytical fragility curves for retrofitted bridges. Earthquake Engineering and Structural Dynamics, vol. 37(8):1157–1174

[14] Choi E., DesRoches R., Nielson B., 2004. Seismic fragility of typical bridges in moderate seismic zones. Engineering Structures, vol. 26: 187–199

[15] Nielson B.G., DesRoches R., 2007. Seismic fragility methodology for highway bridges using a component level approach. Earthquake Engineering and Structural Dynamics, vol. 36(6): 823–839

[16] Ramirez C.M., Miranda E., 2012. Significance of residual drifts in building earthquake loss estimation. Earthquake Engineering and Structural Dynamics, vol. 41(11): 1477–1493

[17] Zhang Y., Fan J., Fan W., 2016. Seismic fragility analysis of concrete bridge piers reinforced by steel fibers. Advances in Structural Engineering, vol. 19(5):837–848

[18] Gardoni P., Mosalam K.M., Kiureghian A.D., 2003. Probabilistic seismic demand models and fragility estimates for RC bridges. Journal of Earthquake Engineering, vol. 7(S1):79–106

[19] Ahmad S., Kyriakides N., Pilakoutas K., et al., 2015. Seismic fragility assessment of existing sub-standard low strength reinforced concrete structures. Earthquake Engineering and Engineering Vibration, vol. 14(3):439–452

[20] FEMA, 2005. HAZUS-MH software, Federal Emergency Management Agency, Washington D.C., USA

[21] Noori H.Z., Amiri G.G., Nekooei M., Zakeri B., 2016. Seismic fragility assessment of skewed MSSS-I girder concrete bridges with unequal height columns. Journal of Earthquake and Tsunami, vol. 10(1):1550013

[22] Hwang H., Liu J.B., Chiu Y.H., 2001. Seismic fragility analysis of highway bridges. Mid-America Earthquake Center report: project MAEC RR-4, University of Illinois at Urbana-Champaign, USA.

[23] Padgett J.E., Nielson B.G., DesRoches R., 2008. Selection of optimal intensity measures in probabilistic seismic demand models of highway bridge portfolios. Earthquake Engineering and Structural Dynamics, vol. 37(5):711–725

[24] Zhang J., Huo Y.L., 2009. Evaluating effectiveness and optimum design of isolation devices for highway bridges using the fragility function method. Engineering Structures, vol. 31(8): 1648–1660.

[25] Shen X., Ye A., Wang X., 2014. Simplified calculation method of elastic-plastic displacement capacity for double-column bent. Journal of Tongji University, vol. 42(4): 513–519 (In Chinese)

[26] Priestley M.J.N., Seible F., Calvi G.M., 1996. Seismic design and retrofit of bridges. John Wiley & Sons, Inc., New York